Solid Solutions of a Jahn–Teller Compound in an Undistorted Host. 3. The Chromium/Zinc Tutton Salt System

Miguel A. Araya,[1a] F. Albert Cotton*,[1b] Lee M. Daniels,[1b] Larry R. Falvello,*,[1c] and Carlos A. Murillo*,[1a,b]

Department of Chemistry, University of Costa Rica, Ciudad Universitaria, Costa Rica, Department of Chemistry and Laboratory for Molecular Structure and Bonding, Texas A&M University, College Station, Texas 77843-3255, and Department of Inorganic Chemistry and Aragon Materials Science Institute, University of Zaragoza-CSIC, 50009 Zaragoza, Spain

Received February 26, 1993®

A series of solid solutions of a Jahn–Teller active compound in an undistorted host has been studied by single-crystal X-ray diffraction. The end members and nine isotypic samples of the Tutton salt system $(NH_4)_2[Cr_xZn_{1-x}(H_2O)_6](SO_4)_2$, with x varying from 0.07 to 0.93, crystallize in the monoclinic space group $P2_1/c$ with $Z = 2$. The unit cell parameters vary slightly with composition, and fall within the following ranges: a, 6.247(1)–6.274(1) Å; b, 12.498(3)–12.531(2) Å; c, 9.239(1)–9.321(2) Å; β, 106.84(1)–106.43(1)°. Except for β, the variations of these parameters are not monotonic at high Cr concentrations. The cell volume falls in the range 690.5(2)–701.7(2) Å^3. The Jahn–Teller distortion at the chromium center changes its direction upon the introduction of as little as 0.07 mole fraction of Zn. With increasing Zn concentration the apparent mean ligand-atom positions describe a distorted octahedral pattern that changes monotonically with concentration. The nature of the mixed systems is examined in terms of the anisotropic displacement tensors, which together with the apparent ligand placement illuminate the magnitude of what may be either static or dynamic disorder. Several interpretations of the results are suggested. The structures of the pure Cr compound on the one hand and all those containing Zn on the other are not genuinely isotypic, because the hydrogen-bonding networks differ.

Introduction

An unpaired e or e_g electron at a transition-metal center almost always leads to an elongation and/or contraction of one or more of the principal axes of the coordination shell.[2] This effect is explained by the Jahn–Teller (J–T) theorem.[3] The examples most frequently encountered in the existing literature are complexes with a d^9 or high-spin d^4 electronic configuration, such as complexes of Cu^{2+} and weak-field Cr^{2+} and Mn^{3+} species.

Jahn–Teller active systems are inherently dynamic. Corresponding to the degeneracy of the unpaired electron in the idealized, symmetrical (tetrahedral or octahedral) molecular prototype, there is a correspondingly degenerate set of distorted shapes which mirrors the actual conformational energy surface of the system. When a Jahn–Teller system is free of a constraining environment, it can be expected to oscillate among the distorted minimum-energy conformations available.

In a limiting environment such as a crystal, however, a Jahn–Teller active system is usually encountered "frozen" into a single distorted geometry, which is presumed to be at or near a conformational potential-energy minimum. It is essential to remember, however, that even in such conditions, the Jahn–Teller active center cannot necessarily be regarded as anything other than a dynamic entity—in this case constrained by its surroundings. Its dynamic nature is usually observed in crystal structures in the form of slightly larger displacements in the appropriate ligands.

Several years ago we reported the results of a study on crystalline mixtures of a Jahn–Teller active molecular system, *trans*-Cr(saccharinate)$_2(H_2O)_4$, in the analogous non-Jahn–Teller active zinc compound.[4] Within a limited concentration range this *molecular* mixture displayed macroscopic properties in accord with those already considered characteristic for solid solutions of extended (i.e., nonmolecular) structural types. In particular, within the appropriate range of composition, strain was a constant function of composition, in accord with Vegard's law. As for microscopic properties, we observed a change of the apparent average molecular shape as a function of composition. As it was further noted that the ligand atoms affected by Jahn–Teller distortion had larger mean-square displacements transverse to the metal–ligand bond than parallel to it, we concluded that the extensive hydrogen bonding present in the system was the mediator of a constraining environment that had caused an adjustment in the shape of the Jahn–Teller active molecule so that it was displaced from a conformational energy minimum.

Since that time, further studies have been undertaken on the response of Jahn–Teller active systems to admixture in the crystalline state with non-Jahn–Teller hosts. The system *trans*-Cr/Zn(nicotinate)$_2(H_2O)_4$[5] presented the fortuitous advantage that the crystallographic symmetries of the pure end members are different: The Cr compound crystallizes in the triclinic system with a large Jahn–Teller distortion in the Cr–O bonds, while the pure Zn compound crystallizes in the monoclinic system with all four Zn–O bonds related by crystallographic symmetry. A calculated superposition of the Cr complex onto the monoclinic Zn structure generated unacceptably short intermolecular contacts. Yet in mixtures with up to 75% Cr, the monoclinic structure was adopted, with very slight changes in the cell dimensions from those of the pure Zn structure. Again it appeared that a change of shape had occurred in the Jahn–Teller system, so that the mixed crystals were not simply static disordered composites of molecules with the shapes of the pure end members. (It is in terms of the latter notion that solid solutions are generally described.[6])

• Abstract published in *Advance ACS Abstracts,* October 1, 1993.

(1) (a) University of Costa Rica. (b) Texas A&M University. (c) University of Zaragoza.

(2) Cotton, F. A.; Wilkinson, G. *Advanced Inorganic Chemistry*, 5th ed., Wiley: New York, 1988.

(3) (a) Jahn, H. A.; Teller, E. *Phys. Rev.* **1936**, *49*, 874. (b) Jahn, H. A.; Teller, E. *Proc. R. Soc. Ser. A* **1937**, *161*, 220.

(4) Cotton, F. A.; Falvello, L. R.; Murillo, C. A.; Valle, G. *Z. Anorg. Allg. Chem.* **1986**, *540/541*, 67.

(5) Cotton, F. A.; Falvello, L. R.; Ohlhausen, E. L.; Murillo, C. A.; Quesada, J. F. *Z. Anorg. Allg. Chem.* **1991**, *598/599*, 53.

0020-1669/93/1332-4853$04.00/0

Table I. Amounts of Reactants Used in the Preparation of Crystalline $(NH_4)_2[Cr_xZn_{1-x}(H_2O)_6](SO_4)_2$[a,b,c]

sample	x(Cr)	no. of mmol Cr^{2+}	no. of mmol Zn^{2+}	tot. vol adjd by water addn, mL
2	0.07(1)	4.7	16	48
3	0.27(1)	8.0	12	45
4	0.48(1)	10.2	1.5	10
5	0.48(1)	11.4	1.0	9
6	0.62(1)	38	7.5	102
7	0.67(1)	42	7.0	110
8	0.66(1)	38	7.5	102
9	0.76(1)	132	10	255
10	0.93(2)	183	7.0	218

[a] Numbers in parentheses are the estimated standard deviations. [b] Samples **6** and **8** were harvested from the same solution. [c] Sample **9** was the second crystalline product of its mother liquor. The first crystals harvested from this mixture were analyzed by atomic absorption spectroscopy as having a composition of x(Cr) of 0.64. Analysis of the second crop gave x(Cr) of 0.74 (essentially the same as that given by X-ray analyses).

We have also encountered a system, $[Cr(H_2O)_6]SiF_6$, in which the central chromium atom sits on a site of crystallographic $\bar{3}$ symmetry, requiring that the six average Cr–O distances be equivalent.[7a] Disorder elsewhere in the structure rendered unreliable (in our opinion) a detailed analysis of displacement parameters, but it is quite possible that signs of Jahn–Teller distortion in dynamic disorder would have been visible in the latter, as was concluded by Stoufer, *et al.*, for the system $[Mn(urea)_6](ClO_4)_3$.[7b]

We report here a series of solid solutions of the ammonium Tutton salts of chromium and zinc. We undertook a study of the Tutton salts both because of our ongoing interest in them (as described in the following paper[8]) and because another Tutton salt mixture, V/Zn, had already been shown capable of forming solid solutions.[9]

As in our previous studies of molecular solid solutions, the results we report here are derived largely from single-crystal X-ray diffraction analyses. We have previously used both "omit maps" and an analysis of displacement tensors in addressing the question of structural homogeneity. In this study we have also examined the displacement parameters in an attempt to illuminate as far as possible the effects of a constraining crystalline environment on the coordination geometry about the composite Cr/Zn site.

Experimental Section

In the preparation of divalent chromium compounds all operations were carried out under a nitrogen atmosphere by using standard techniques. Water was deionized, deoxygenated by prolonged refluxing in a nitrogen atmosphere, and distilled just before it was used. The pure chromium and zinc salts were prepared as described in the following paper.[8] Atomic absorption analyses were carried out on a Shimadzu A670 spectrophotometer.

Preparation of Crystalline $(NH_4)_2[Cr_xZn_{1-x}(H_2O)_6](SO_4)_2$. Crystals were prepared by mixing either weighed portions of the pure chromium and zinc Tutton salts or their solutions and adjusting the total volume by addition of water. To each of the solutions a few drops of ethanol (less than 0.4 mL) were added. They were then cooled to 5 °C. The relative concentrations of the solutions used are shown in Table I.

To minimize the possibility of the formation of inhomogeneous crystals, samples were collected as soon as they reached an adequate size for X-ray diffraction analysis, normally when there were just a few crystals in the flask.

X-ray Structure Analyses. Diffraction data were collected on nine crystalline samples of $(NH_4)_2[Cr_xZn_{1-x}(H_2O)_6](SO_4)_2$ having seven different compositions. Data sets for samples **2–9** were all collected on the same P3/F (Equivalent) diffractometer. The data for sample **10** were collected on a CAD4 diffractometer. All of the data sets were collected at the same (controlled) room temperature, 22 ± 1 °C. For each data set an almost colorless (low Cr content) to pale-blue (higher Cr content) crystal was mounted on the tip of a glass fiber. The orientation of each sample was initially determined from reflections taken from a 360° ϕ-rotation photograph. The same set of 24 or 25 known reflections was then used for each sample for the determination of accurate lattice dimensions. For all but one of the samples, intensity data were collected in the $+h,+k,\pm l$ quadrant; for sample **9** the $+h,\pm k,\pm l$ hemisphere was collected. Since our P3/F diffractometer (a 1984 Nicolet modification of an early model Syntex P$\bar{1}$ instrument from what, as of this writing, is now the Siemens family of diffractometers) has no facility for attenuation of the beam, very strong reflections flood the detector and are recorded with zero intensity (and therefore are not used in the structure refinement). For each of the crystals studied on this instrument, several (2–10) strong reflections were skipped in this manner. We could have avoided this problem by choosing much smaller crystals. However, we chose to give up a few low-angle strong reflections in order to gain many more significant observations at higher values of $(\sin\theta)/\lambda$. Lorentz and polarization corrections were applied to each data set, and equivalent data were averaged. For each data set a ψ-scan absorption correction was applied. In the full-matrix least-squares refinement of the structures, all data with nonnegative measured intensities were used. The structural models were refined on F_o^2. Additional crystallographic data are summarized in Table II.

Starting positional parameters for the non-hydrogen atoms were taken from the literature.[8] An initial value for the parameter describing the Cr/Zn ratio at the metal site was based in each case on the chemical analysis for that sample. Hydrogen atom positions were found in difference Fourier maps. The model refined in each case included anisotropic temperature factors for the non-hydrogen atoms and a variable independent isotropic temperature factor for each hydrogen atom.

As a check on the stability of the composition parameter for the metal atom site, its value was arbitrarily changed to values both significantly higher and lower than the expected value. In every case the parameter returned to the same value. We have discussed the validity of determining the Cr/Zn ratio in the sample crystal using single-crystal X-ray diffraction in a previous report.[4]

Refinement calculations were carried out on a Local Area VAX cluster using the program SHELXL-93.[10] Final non-hydrogen positional parameters and the composition parameter for each sample are given in Table III. Table IV contains the metal-oxygen bond distances for each sample, as well as data related to the displacement parameters at the oxygen-atom sites (*vide infra*).

We re-refined the structures of the pure Cr and pure Zn compounds (reported in the following paper[8]) using the same techniques, in order to permit a consistent comparison with the mixed systems. For the pure Zn Tutton salt only, we found it necessary to apply similarity restraints, pairwise, for the three geminal O–H pairs, a similarity restraint for the three H–O–H angles, and one similarity restraint for the four N–H distances. (These enter the refinement as observations.) In addition, the two hydrogen atoms attached to atom O(3) were constrained to have the same displacement parameters.

Analyses of the anisotropic displacement parameters for all of the samples were conducted with the programs ORFFE[11] and THMA11.[12] We examined the results of a combined translation–libration tensor analysis[13] (usually called a TLS treatment) for various models involving overall libration and translation as well as different combinations of independent motions of the $[M(H_2O)_6]^{2+}$ and SO_4^{2-} groups. Differences in mean-square displacement amplitudes (ΔMSDA values) along inter-

(6) See, for example: (a) West, A. R. *Solid State Chemistry and its Applications*, Wiley, New York, 1984; Chapter 10, pp 358–373. (b) Reinen, D. *J. Solid State Chem.* **1979**, *27*, 71. (c) Guen, L.; Nguyen-Huy-Dung *Acta Crystallogr.* **1976**, *B32*, 311. (d) Jirák, Z.; Vratislav, S.; Novák, P. *Phys. Status Solidi* **1978**, *50*, K21.
(7) (a) Cotton, F. A.; Falvello, L. R.; Murillo, C. A.; Quesada, J. F. *J. Solid State Chem.* **1992**, *96*, 192. (b) Aghabozorg, H.; Palenik, G. J.; Stoufer, R. C.; Summers, J. *Inorg. Chem.* **1982**, *21*, 3903.
(8) Cotton, F. A.; Daniels, L. M.; Murillo, C. A.; Quesada, J. F. *Inorg. Chem.*, following paper in this issue and references therein.
(9) Deeth, R. J.; Figgis, B. N.; Forsyth, J. B.; Kucharski; E. S.; Reynolds, P. A. *Aust. J. Chem.* **1988**, *41*, 1289.
(10) (a) Sheldrick, G. M. SHELXL-93: FORTRAN-77 program for the refinement of crystal structures from diffraction data. University of Göttingen, 1993. (b) Sheldrick, G. M. *J. Appl. Crystallogr.*, in press.
(11) Bussing, W. R., Martin, K. O.; Levy, H. A. ORFFE: A crystallographic function and error program. Oak Ridge National Laboratory, 1971.
(12) (a) Dunitz, J. D.; Schomaker, V.; Trueblood, K. N. *J. Phys. Chem.* **1988**, *92*, 856. (b) Trueblood, K. N.1992. Private communication.
(13) Schomaker, V.; Trueblood, K. N. *Acta Crystallogr.* **1968**, *B24*, 63.

Table II. Crystal Data for $(NH_4)_2[Cr_xZn_{1-x}(H_2O)_6](SO_4)_2$

	1	2	3	4	5	6	7	8	9	10	11
formula	$Cr_xZn_{1-x}S_2O_{14}N_2H_{20}$										
x(Cr) (molar fraction)	0	0.07(1)	0.27(1)	0.48(1)	0.48(1)	0.62(1)	0.67(1)	0.66(1)	0.76(1)	0.93(2)	1
fw	401.66	400.73	398.05	395.24	395.24	393.36	392.70	392.83	391.49	389.22	388.28
space group	$P2_1/c$										
a, Å	6.254(2)	6.247(1)	6.256(1)	6.2654(7)	6.267(1)	6.273(2)	6.273(1)	6.274(1)	6.2724(8)	6.263(2)	6.200(1)
b, Å	12.500(4)	12.498(3)	12.507(2)	12.514(2)	12.525(2)	12.523(3)	12.528(2)	12.517(3)	12.531(2)	12.524(2)	12.703(2)
c, Å	9.224(2)	9.239(1)	9.255(1)	9.279(2)	9.281(1)	9.297(2)	9.300(1)	9.303(2)	9.312(1)	9.321(2)	9.431(1)
β, deg	106.87(2)	106.84(1)	106.74(1)	106.64(1)	106.65(1)	106.56(2)	106.55(1)	106.54(2)	106.51(1)	106.43(1)	106.66(1)
V, Å^3	690.1(3)	690.5(2)	693.4(2)	697.1(1)	697.9(2)	700.3(3)	700.6(2)	700.3(3)	701.7(2)	701.3(3)	711.5(2)
Z	2										
d_{calcd}, g/cm^3	1.933	1.927	1.906	1.883	1.881	1.865	1.861	1.863	1.853	1.843	1.812
μ(Mo Kα), cm^{-1}	21.80	21.08	18.97	16.77	16.75	15.29	14.79	14.89	13.87	12.18	11.32
radiation	Mo Kα ($\lambda_{\bar{\alpha}}$ = 0.710 73 Å) monochromated in incident beam										
temp, °C	22(1)										
transm factors											
max	0.9982	0.9991	0.9972	0.9999	0.9970	0.9966	0.9957	0.9943	0.9995	1.0000	0.9979
min	0.7802	0.8600	0.7989	0.8798	0.7811	0.8139	0.8153	0.9112	0.8127	0.9083	0.9385
R^a	0.032	0.022	0.021	0.022	0.022	0.030	0.022	0.027	0.025	0.048	0.023
$wR2^{b,c}$	0.088	0.062	0.059	0.059	0.063	0.075	0.058	0.068	0.061	0.134	0.063

[a] $R = \sum||F_o| - |F_c||/\sum|F_o|$. [b] $wR2 = [\sum w(F_o^2 - F_c^2)^2/\sum w(F_o^2)^2]^{1/2}$. [c] Weighting function, $w = [\sigma^2(F_o^2) + (p_1(\max(F_o^2,0) + 2F_c^2)/3)^2 + p_2(\max(F_o^2,0) + 2F_c^2)/3]^{-1}$; p_1 and p_2 are set individually for each refinement.

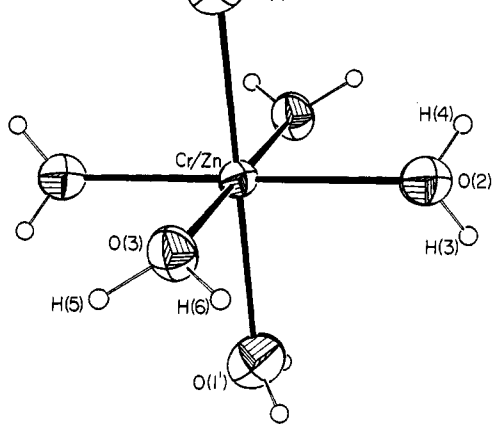

Figure 1. ORTEP drawing of the $[Cr_{0.66}Zn_{0.34}(H_2O)_6]^{2+}$ ion indicating the amplitudes of anisotropic thermal motion for the non-hydrogen atoms. The thermal ellipsoids are drawn at the 50% probability level. Hydrogen atoms are shown as arbitrarily-sized spheres.

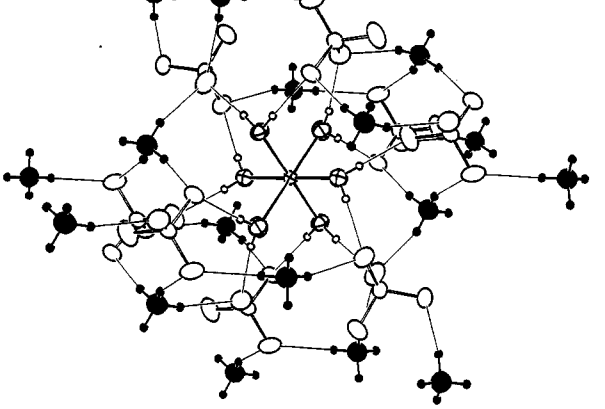

Figure 2. Representation of the hydrogen-bond network in the Cr/Zn Tutton salts. Each of the water ligands (center of the drawing) have hydrogen bonds to two sulfate groups (open ellipsoids), which in turn participate in hydrogen bonds to ammonium ions (dark ellipsoids) and to other water ligands.

atomic vectors were computed by the program THMA11 for all pairs of non-hydrogen atoms in a set comprising the atoms of the basic asymmetric unit and all atoms hydrogen-bonded to those of the basic asymmetric unit. This provided a rigid-bond test[14] for the hexaaquametal and sulfate groups, as well as ΔMSDA values for the independent hydrogen bonds.

Results and Discussion

General Observations. A series of nine crystal structures of solid solutions with the general formula $(NH_4)_2[Cr_xZn_{1-x}(H_2O)_6](SO_4)_2$ with compositions varying from $x = 0.07$ to $x = 0.93$ were studied. They crystallize in the same space group as the pure end members for which the structures are reported in detail in the following paper. An ORTEP drawing of the parent complex cation is given in Figure 1. As shown in Figure 2, the structures are held together by an extensive network of hydrogen bonds. The cation, $[M(H_2O)_6]^{2+}$, resides on an inversion center. As can be seen in Figure 3, the M–O(3) bond distance is virtually unaffected by the formation of the solid solutions; it remains essentially constant. The other two unique M–L bonds, M–O(1) and M–O(2), show relatively smooth increases in evident length—that is, in the distance between the mean metal position and the apparent mean oxygen position–up to a composition of x(Cr) = 0.93. However, when x(Cr) = 1.00, there is a dramatic change in those distances, coupled with a change in the hydrogen bonding pattern. The changes are such that M–O(1) becomes smaller by *ca.* 0.09 Å and M–O(2) increases by *ca.* 0.15 Å.[15]

Composition. The composition was determined in each case by X-ray diffraction. The populations were established by refinements in which the Cr/Zn site was treated as a compound scatterer. The differences in the magnitude and shape of the scattering factors of chromium and zinc, as described in our previous papers[4,5] served as a basis for a stable and determinate refinement. For those samples for which just a few crystals were produced, the composition was also checked by atomic absorption spectroscopy. In all cases, the composition derived from X-ray diffraction analysis and that from atomic absorption studies were the same, within 3 standard deviations. In one case, we analyzed two crystals produced from the same solution, namely those

(14) Hirshfeld, F. L. *Acta Crystallogr.* **1976**, *A32*, 239.

(15) It has been established that the Jahn–Teller distortion, which can occur in either of the mutually perpendicular directions, can be switched between these directions by pressure in the deuterated copper Tutton salt. Schultz, A. J.; Simmons, C. J.; Hitchman, M. A. Private Communication. There is also a temperature dependence of the structure found in that system. Hathaway, B. J.; Hewat, A. W. *J. Solid State Chem.* **1984**, *51*, 364.

Table III. Positional and Equivalent Isotropic Displacement Parameters for the Non-Hydrogen Atoms of the Cr_xZn_{1-x} Tutton Salts[a]

atom	x	y	z	U_{eq}	x(Cr)	atom	x	y	z	U_{eq}
Zn	0	0	0	19(1)	**0**	S	−2603(1)	3632(1)	−924(1)	20(1)
Cr/Zn	0	0	0	19(1)	**0.07(1)**	S	−2599(1)	3630(1)	−924(1)	20(1)
Cr/Zn	0	0	0	20(1)	**0.27(1)**	S	−2594(1)	3626(1)	−924(1)	22(1)
Cr/Zn	0	0	0	20(1)	**0.48(1)**	S	−2589(1)	3623(1)	−923(1)	24(1)
Cr/Zn	0	0	0	20(1)	**0.48(1)**	S	−2588(1)	3622(1)	−924(1)	24(1)
Cr/Zn	0	0	0	20(1)	**0.62(1)**	S	−2584(1)	3619(1)	−925(1)	25(1)
Cr/Zn	0	0	0	21(1)	**0.67(1)**	S	−2581(1)	3618(1)	−925(1)	26(1)
Cr/Zn	0	0	0	20(1)	**0.66(1)**	S	−2582(1)	3618(1)	−925(1)	25(1)
Cr/Zn	0	0	0	20(1)	**0.76(1)**	S	−2580(1)	3615(1)	−928(1)	26(1)
Cr/Zn	0	0	0	21(1)	**0.93(2)**	S	−2575(2)	3610(1)	−939(1)	28(1)
Cr	0	0	0	21(1)	**1**	S	−2567(1)	3586(1)	−1045(1)	24(1)
O(1)	1652(4)	1088(2)	1709(3)	27(1)	**0**	O(2)	354(4)	1115(2)	−1624(3)	28(1)
O(1)	1663(3)	1087(1)	1710(2)	28(1)	**0.07(1)**	O(2)	342(3)	1114(1)	−1633(2)	28(1)
O(1)	1684(2)	1099(1)	1722(2)	32(1)	**0.27(1)**	O(2)	327(2)	1115(1)	−1644(2)	30(1)
O(1)	1701(3)	1110(1)	1732(2)	37(1)	**0.48(1)**	O(2)	316(3)	1118(1)	−1654(2)	33(1)
O(1)	1708(2)	1110(1)	1735(2)	36(1)	**0.48(1)**	O(2)	314(2)	1119(1)	−1655(1)	32(1)
O(1)	1722(3)	1121(2)	1745(2)	39(1)	**0.62(1)**	O(2)	309(3)	1121(2)	−1664(2)	34(1)
O(1)	1729(3)	1122(1)	1747(2)	39(1)	**0.67(1)**	O(2)	306(3)	1124(1)	−1670(2)	35(1)
O(1)	1728(3)	1124(2)	1751(2)	39(1)	**0.66(1)**	O(2)	308(3)	1121(1)	−1667(2)	35(1)
O(1)	1736(2)	1128(1)	1753(2)	40(1)	**0.76(1)**	O(2)	302(2)	1127(1)	−1678(1)	36(1)
O(1)	1762(7)	1130(3)	1754(4)	43(1)	**0.93(2)**	O(2)	318(7)	1137(3)	−1697(4)	40(1)
O(1)	1715(3)	1069(1)	1673(2)	39(1)	**1**	O(2)	411(3)	1167(1)	−1802(2)	39(1)
O(3)	3009(3)	−682(3)	5(3)	25(1)	**0**	O(4)	−4085(4)	2711(3)	−881(3)	33(1)
O(3)	3003(2)	−680(1)	3(2)	26(1)	**0.07(1)**	O(4)	−4090(2)	2719(1)	−880(2)	34(1)
O(3)	2985(2)	−685(1)	−14(2)	27(1)	**0.27(1)**	O(4)	−4079(2)	2714(1)	−883(2)	37(1)
O(3)	2967(2)	−688(1)	−28(2)	29(1)	**0.48(1)**	O(4)	−4069(2)	2710(1)	−889(2)	39(1)
O(3)	2967(2)	−688(1)	−30(1)	28(1)	**0.48(1)**	O(4)	−4068(2)	2709(1)	−889(2)	38(1)
O(3)	2956(3)	−690(2)	−39(2)	29(1)	**0.62(1)**	O(4)	−4062(3)	2705(2)	−896(2)	40(1)
O(3)	2951(2)	−691(1)	−41(2)	30(1)	**0.67(1)**	O(4)	−4055(2)	2703(1)	−896(2)	41(1)
O(3)	2953(2)	−694(1)	−42(2)	29(1)	**0.66(1)**	O(4)	−4055(3)	2704(1)	−892(2)	40(1)
O(3)	2942(2)	−696(1)	−50(1)	29(1)	**0.76(1)**	O(4)	−4053(2)	2699(1)	−902(2)	41(1)
O(3)	2929(5)	−699(3)	−60(4)	31(1)	**0.93(2)**	O(4)	−4039(6)	2695(3)	−915(4)	44(1)
O(3)	2966(2)	−714(1)	1(2)	28(1)	**1**	O(4)	−4012(2)	2657(1)	−1094(2)	41(1)
O(5)	−2151(4)	4244(3)	480(2)	40(1)	**0**	O(6)	−3769(3)	4325(2)	−2204(2)	27(1)
O(5)	−2153(3)	4235(1)	482(2)	42(1)	**0.07(1)**	O(6)	−3761(2)	4329(1)	−2202(1)	27(1)
O(5)	−2170(3)	4232(1)	476(2)	45(1)	**0.27(1)**	O(6)	−3747(2)	4323(1)	−2196(1)	29(1)
O(5)	−2179(3)	4227(1)	473(2)	48(1)	**0.48(1)**	O(6)	−3733(2)	4321(1)	−2194(1)	31(1)
O(5)	−2183(3)	4226(1)	471(1)	47(1)	**0.48(1)**	O(6)	−3833(2)	4319(1)	−2193(1)	30(1)
O(5)	−2192(4)	4221(2)	466(2)	48(1)	**0.62(1)**	O(6)	−3718(3)	4315(1)	−2189(2)	31(1)
O(5)	−2194(3)	4221(1)	465(2)	50(1)	**0.67(1)**	O(6)	−3717(2)	4315(1)	−2191(2)	32(1)
O(5)	−2189(3)	4223(2)	466(2)	49(1)	**0.66(1)**	O(6)	−3719(2)	4315(1)	−2193(2)	31(1)
O(5)	−2204(3)	4217(1)	460(1)	49(1)	**0.76(1)**	O(6)	−3713(2)	4312(1)	−2193(1)	32(1)
O(5)	−2214(7)	4208(3)	446(4)	52(1)	**0.93(2)**	O(6)	−3701(5)	4308(2)	−2200(3)	34(1)
O(5)	−2285(3)	4145(1)	349(1)	45(1)	**1**	O(6)	−3710(2)	4292(1)	−2280(1)	31(1)
O(7)	−502(3)	3221(3)	−1151(3)	30(1)	**0**	N	3579(5)	3484(4)	1364(4)	30(1)
O(7)	−497(2)	3230(1)	−1151(2)	31(1)	**0.07(1)**	N	3578(3)	3478(2)	1343(2)	31(1)
O(7)	−485(2)	3228(1)	−1144(2)	33(1)	**0.27(1)**	N	3579(3)	3484(2)	1335(2)	32(1)
O(7)	−478(2)	3226(1)	−1137(2)	36(1)	**0.48(1)**	N	3579(3)	3487(2)	1331(2)	34(1)
O(7)	−473(2)	3228(1)	−1133(1)	35(1)	**0.48(1)**	N	3578(3)	3487(1)	1329(2)	33(1)
O(7)	−467(3)	3228(1)	−1133(2)	36(1)	**0.62(1)**	N	3586(4)	3492(2)	1326(3)	35(1)
O(7)	−470(2)	3227(1)	−1134(2)	37(1)	**0.67(1)**	N	3588(3)	3495(2)	1328(2)	35(1)
O(7)	−465(2)	3227(1)	−1132(2)	36(1)	**0.66(1)**	N	3585(4)	3493(2)	1325(3)	35(1)
O(7)	−458(2)	3229(1)	−1127(1)	37(1)	**0.76(1)**	N	3590(3)	3498(1)	1323(2)	35(1)
O(7)	−448(5)	3232(3)	−1132(4)	39(1)	**0.93(2)**	N	3589(8)	3507(4)	1297(6)	38(1)
O(7)	−361(2)	3262(1)	−1207(2)	35(1)	**1**	N	3658(3)	3571(2)	1269(2)	34(1)

[a] The equivalent isotropic displacement parameter U_{eq} (in Å^2) is calculated as $\sum U_{ij}\mathbf{a}_i\mathbf{a}_j a_i^* a_j^*$; $i, j = 1, 3$. For each atomic site, the coordinates are given for all eleven samples in the study. The coordinates are ($\times 10^4$) and the displacement parameters are (Å $\times 10^3$).

designated as **6** and **8**. Their compositions were similar, thus giving supporting evidence of the homogeneity of the samples.

Displacement Parameters. The anisotropic displacement parameters derived from the diffraction data for this series of Tutton salts provide useful insight into what may be either dynamic or static effects accompanying the observed progression of geometrical distortion. (That it is possible to derive useful information on dynamics even from data taken in more or less routine fashion has been demonstrated by Bürgi and Stebler.[16]) We shall focus on the differences in mean-square displacement amplitudes (ΔMSDA) along interatomic vectors and on the magnitudes and directions of principal displacements, which yield in this case the most useful information.[17]

Table V shows the difference MSDA values for all pairs of non-hydrogen atoms within a set consisting of one asymmetric unit and all of the atoms hydrogen-bonded to that asymmetric unit, for the structure of sample **8**, with $x(Cr) = 0.66(1)$. The numbers in this table are quite representative of those found for

(16) Stebler, M.; Bürgi, H. B. *J. Am. Chem. Soc.* **1987**, *109*, 1395.

(17) Since the crystallographic asymmetric unit comprises three chemically distinct entities joined by hydrogen bonds, we did not expect useful results from an overall TLS analysis. While we were able to achieve residuals in the range of 10% for the overall TLS refinement, the results do not contribute to our understanding of the system. It is possible to derive clearly defined translation and libration tensors individually for the SO_4^{2-} groups and, to a lesser extent, for the $[M(H_2O)_6]^{2+}$ units.

Table IV. M–O Distances, ΔMSDA Values, and Magnitudes and Relative Directions of the Largest Root-Mean-Square Displacements for the Ligand Oxygen Atoms in the Series $(NH_4)_2[Cr_xZn_{1-x}(H_2O)_6](SO_4)_2$[a]

		M–O(1)				M–O(2)				M–O(3)			
	x(Cr)	d	ΔMSDA	RMS_{max}	angle	d	ΔMSDA	RMS_{max}	angle	d	ΔMSDA	RMS_{max}	angle
1	0	2.111(2)	22	0.204(4)	89(3)	2.104(3)	65	0.189(4)	58(6)	2.065(2)	3	0.176(3)	81(6)
2	0.07(1)	2.114(1)	42	0.199(2)	75(1)	2.108(1)	20	0.194(2)	76(2)	2.059(1)	30	0.179(2)	75(3)
3	0.27(1)	2.138(1)	113	0.210(2)	66(2)	2.117(1)	53	0.202(2)	70(2)	2.058(1)	27	0.188(2)	75(2)
4	0.48(1)	2.161(2)	171	0.221(2)	58(2)	2.127(1)	99	0.209(2)	64(2)	2.056(1)	37	0.196(2)	74(2)
5	0.48(1)	2.164(1)	169	0.221(2)	58(2)	2.130(1)	95	0.206(2)	64(2)	2.057(1)	36	0.191(1)	75(2)
6	0.62(1)	2.184(2)	219	0.230(3)	54(3)	2.139(2)	143	0.211(3)	55(3)	2.055(2)	47	0.195(2)	77(3)
7	0.67(1)	2.188(2)	212	0.230(2)	56(2)	2.145(2)	148	0.220(2)	58(2)	2.054(1)	50	0.197(2)	73(2)
8	0.66(1)	2.191(2)	228	0.231(2)	53(2)	2.141(2)	152	0.220(3)	56(2)	2.057(1)	39	0.194(2)	73(2)
9	0.76(1)	2.199(1)	240	0.240(2)	52(1)	2.153(1)	164	0.220(2)	53(2)	2.053(1)	36	0.199(1)	75(1)
10	0.93(2)	2.207(4)	280	0.244(5)	45(5)	2.179(4)	243	0.235(6)	51(5)	2.048(3)	24	0.210(4)	75(4)
11	1	2.121(1)	137	0.253(2)	68(1)	2.324(2)	181	0.232(2)	51(2)	2.050(1)	37	0.188(2)	79(2)

[a] The four entries for each M–O bond are as follows (from left to right): (1) M–O distance in Å; (2) ΔMSDA value ($\times 10^4$) along the M–O bond, MSDA(O) − MSDA(M), in $Å^2$ (MSDA = mean square displacement amplitude); (3) for the oxygen atom, largest principal root-mean-square displacement, in Å; (4) angle between the M–O bond and the direction of the oxygen-atom largest root-mean-square displacement, in degrees.

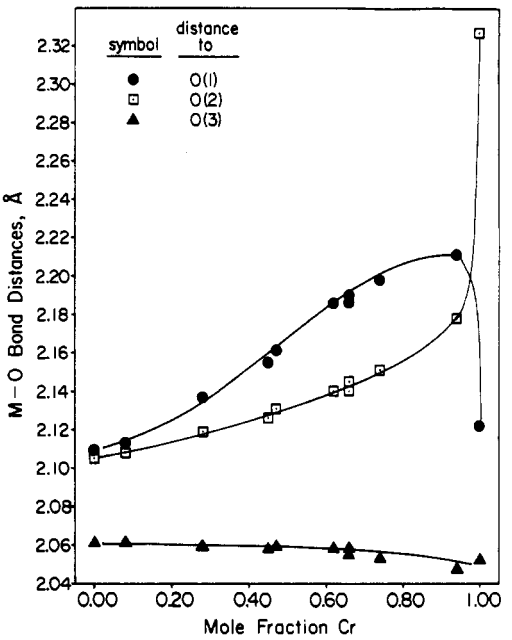

Figure 3. Plot of the three independent metal-to-oxygen bonds in the $[Cr_xZn_{1-x}(H_2O)_6]^{2+}$ ions versus the mole fraction of Cr. The values for 100% Cr correspond to a change in the hydrogen bonding pattern.

all of the samples, which, with just one exception (*vide infra*), show an identical pattern.

The first noteworthy feature of Table V involves the ΔMSDA values for the S–O bonds of the sulfate group. In line with the ideas underlying the "rigid bond test"[14] these four values should be small. This criterion is well satisfied by all of the samples. This provides an indication that the diffraction data are capable of defining the finer features of these structures.

We also note a systematic diminution of the ΔMSDA values for pairs of atoms involved in hydrogen bonds. These effects are not as pronounced as the ΔMSDA values for the S–O covalent bonds, but the fact that the systematically lower ΔMSDA values for H-bonded pairs comprise a constant, inviolate feature of all of the structures, leads us to conclude that the hydrogen bonding does indeed mediate an enhanced rigidity of the extended structure. The bifurcated hydrogen bond involving N as donor and O4B and O4C as acceptor atoms (Table V) is, not surprisingly, the only exception to the trend. We also note the presence of a number of small ΔMSDA values for pairs of atoms not involved in hydrogen bonding.

Table V shows another feature of considerable interest. For O(1), O(2), and O(3)—the atoms bound to the metal center—the ΔMSDA values for the hydrogen bonds are significantly smaller in each case than is the value for the respective M–O bond. This is true not only for the M–O(1) and M–O(2) bonds, which are the ones that vary in observed length with concentration, but also for M–O(3), the most rigid of the three M–O bonds. The general trend is violated only in the pure Zn sample and the sample with x(Cr) = 0.07, and (by 0.0004 $Å^2$) for one of the H-bonds involving atom O(3) in sample **10**.

Not only does this trend in the ΔMSDA values for H-bonded pairs serve to highlight the effects of hydrogen bonding on the extended structure, it also points to perhaps the most telling trend in the whole series—an essentially monotonic increase in ΔMSDA for M–O(1) and M–O(2) as a function of x(Cr). In the samples with x(Cr) = 0 and 0.07, the ΔMSDA values for the M–O vectors do not suggest the presence of any special effects. With increasing x(Cr), however, a pronounced increase of ΔMSDA accompanies the increase in the apparent M–O distance, for M–O(1) and M–O(2). This trend is reversed only for the pure-Cr sample.

In Table IV are given the M–O bond lengths and respective ΔMSDA values for all of the samples. While the M–O pairs of the $[M(H_2O)_6]^{2+}$ moiety show an unmistakable increase in difference mean-square displacements parallel to the M–O vectors, these directions are *not* the ones in which the oxygen sites are principally elongated as a function of composition. Table IV also gives, for each ligand oxygen atom in each sample, its largest root-mean-square displacement ($Rmsd_{max}$ in Å) and the angle between the direction of that displacement and the respective M–O bond. Atoms O(1) and O(2) display noticeable increases in the values of $Rmsd_{max}$ with increasing mole fraction of Cr. For atom O(1), the *direction* of the largest Rmsd also shows a distinct trend. In the pure Zn sample, this direction is perpendicular to the Zn–O(1) bond, lies very near (about 9° out of) the Zn,O(1),O(2) plane, and makes an angle of approximately 7° with the direction of the Zn–O(2) bond. As x(Cr) increases, the direction of maximum displacement is rotated in the M,O(1),O(2) plane until the angle it makes with the M–O(1) vector reaches a value of 45° for x(Cr) = 0.93. (In the pure Cr Tutton salt structure, which is not isotypic, the value of this angle is 68°.) These data are represented graphically in Figure 4, in which 60% displacement ellipsoids for M and O(1) are drawn in nonperspective projection on the M,O(1),O(2) plane for the whole series of mixtures. The progressive change in the magnitude and direction of the largest principal displacement at O(1) is clearly seen from the figure.

Atom O(2) shows a similar increase in the value of its largest principal displacement with increasing x(Cr). There is an observable trend in the orientation of the principal axes; but unlike those of O(1), the principal displacement directions for O(2) are not related to the principal planes of the overall cation structure. So, while the largest principal displacement of O(1) remains near the M,O(1),O(2) plane in all of the samples, the largest principal displacement of O(2) is well out of that plane in every case. The

Table V. ΔMSDA Values for **8**, Ammonium Cr/Zn Tutton Salt, with $x(Cr) = 0.66(1)$[a]

	O7A	O6C	O6B	O6A	O5A	O4C	O4B	O4A	N	O(7)	O(6)	O(5)	O(4)	O(3)	O(2)	O(1)	S
Cr/Zn	226	159	115	88	57	36	149	133	163	126	60	261	133	39	152	228	35
S	257	89	74	161	247	94	247	80	107	5	5	5	−9	9	49	184	
O(1)	(45)	−191	−96	(74)	−90	−108	−23	−65	−171	−77	−174	44	26	−119	−77		
O(2)	131	80	0	−6	(9)	−130	155	−26	67	(47)	−5	101	58	−44			
O(3)	116	60	(9)	−156	58	−44	−47	(8)	77	55	26	201	110				
O(4)	2	−18	−89	14	−38	0	18	0	−12	−18	7	37					
O(5)	−1	−283	−104	−95	178	−179	−35	−120	−258	−27	0						
O(6)	253	0	24	134	236	28	246	30	82	6							
O(7)	23	−39	−2	56	1	90	130	−22	(−13)								
N	15	(−14)	−122	15	−9	(211)	(219)	−46									
O4A	−113	−9	35	−164	88	0	−195										
O4B	−90	−164	−159	7	−150	−61											
O4C	−45	−157	−164	35	35												
O5A	159	−31	−283	−53													
O6A	−51	−47	0														
O6B	125	128															
O6C	2																

[a] The value listed is 10^4 MSDA for the column atom minus that for the row atom, in the direction of the interatomic vector. Values for hydrogen-bonded pairs are given in parentheses. O7A is O(7) at $(x, 0.5 - y, 0.5 + z)$; O4A is O(4) at $(-x, -y, -z)$; O4B is O(4) at $(1 + x, 0.5 - y, 0.5 + z)$; O4C is O(4) at $(1 + x, y, z)$; O5A is O(5) at $(x, 0.5 - y, -0.5 + z)$; O6A is O(6) at $(1 + x, 0.5 - y, 0.5 + z)$; O6B is O(6) at $(-x, -0.5 + y, -0.5 - z)$; O6C is O(6) at $(-x, 1 - y, -z)$.

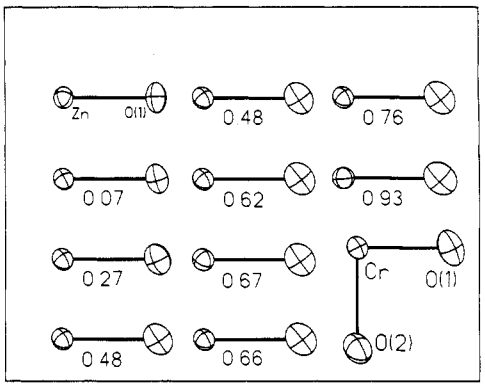

Figure 4. 60% displacement ellipsoids for the metal and O(1) sites, for the nine Cr/Zn mixed Tutton salts and the two end members. The plots are drawn to approximately the same scale, in nonperspective projection on the M, O(1), O(2) plane. For the chromium end member, which is not isotypic with the rest, atom O(2) is also shown. For the mixed Cr/Zn structures, the mole fraction of Cr is given.

displacement ellipsoid of atom O(2) is shown in Figure 4 for the pure Cr sample, in which the Cr–O(2) bond is the one elongated by Jahn–Teller distortion.

Atom O(3) shows no realignment of its principal displacements as a function of composition. Along with the relative constancy of the M–O(3) ΔMSDA value, this implies that changing composition does not cause significant structural change relative to the M–O(3) direction.

Atom O(3) does, however, display a general increase in displacement with increasing $x(Cr)$, as does the structure as a whole. We would normally be hesitant to compare the absolute magnitudes of displacement parameters from one structure to another, even for such similar structures with data gathered under such similar conditions. We see in this case, however, that with the exception of the generally poorly behaved sample **10**, the ΔMSDA values for the sulfate group remain very similar throughout the series—even as the values of the displacement parameters for most of the atoms involved show an upward trend with increasing $x(Cr)$. For this reason, the general increase in displacement with $x(Cr)$ appears to be significant, as are the more pronounced effects seen for the individual atoms O(1) and O(2).

Disorder and Observed Geometry. The feature of most fundamental interest in the mixed Cr/Zn ammonium Tutton salts is the crystallographic equivalence of the sites occupied by $[Cr(H_2O)_6]^{2+}$ and those occupied by $[Zn(H_2O)_6]^{2+}$. The fact that zinc and chromium atoms occupy crystallographically equivalent centers of symmetry, in static disorder, suggests a number of implications for the results of diffraction studies. First of all, as a chromium atom would be expected to have more vibrational motion than a zinc atom, the displacement parameters for the metal atom site could at first glance be expected to be a compromise between the two. However, since the data were all taken at room temperature, librational and translational effects undoubtably dominate the displacement parameters of the metal site.

Of somewhat more interest are the effects of solid solution formation on the water ligands bonded to the chromium and zinc atoms. On one hand, the oxygen atoms of these ligands participate in largely covalent and presumably strong bonds to the chromium and zinc centers, forming Cr and Zn complexes with distinct shapes. On the other hand, on incorporation into a Tutton salt crystal, the oxygen ligands of the hexaaquametal complex also take part in hydrogen bonds that stabilize the crystal structure (Figure 2). In a stable crystalline mixture of the Cr and Zn Tutton salts, either these two countervailing influences on the water ligands must be balanced, or else one of them must dominate. If the molecular shapes of the end members were to dominate the situation, the ligand affected by Jahn–Teller distortion in the Cr complex and not in the Zn complex would be in static disorder in the mixed crystals. Such a disorder would be visible either in the displacement parameters or, in a favorable case, in a separation of the atomic centers observed by diffraction. At the opposite extreme, if the hydrogen bonding dominates the energetics of the mixed crystals, one or both of the Cr and Zn complexes would suffer a change of shape in adapting to the crystalline environment. In this case a measure of dynamic disorder would almost certainly remain, but the potential energy surface influencing an oxygen atom ligated to zinc and that for an atom bonded to chromium would have their minima at crystallographically equivalent points. Between the two extremes lie a host of possibilities, all involving a combination of static and dynamic disorder, including the possibility that the nature of the mixtures changes at some composition.

In the systems we report here, the ligand oxygen atoms O(1) and O(2) are both affected by the formation of crystalline mixtures, in terms of their evident positions and their displacement parameters. It is for atom O(1) that the changes are more systematically related to composition, as Table IV and Figure 4 show. Yet in the end-member Cr and Zn Tutton salts, the M–O(1) distances differ by only 0.01 Å. In the mixed-composition crystals, the Jahn–Teller distortion at the chromium center is switched, and it is the distortion-switched complex that must serve as a point of departure for considering the mixed systems.

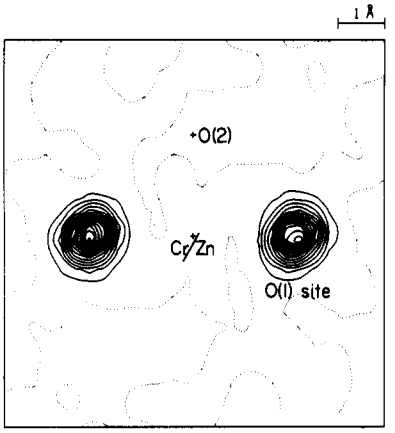

Figure 5. Contoured difference Fourier map in the plane defined by the (Cr/Zn), O(1), and O(2) sites for sample **8**. The values of F_{calc} for this map were from a model containing all atoms except O(1).

From this point, the diffraction data do not distinguish well among the several possibilities. We present several possible interpretations here, along with various considerations relevant to each.

(a) Fully Static Disorder. The displacement ellipsoids shown in Figure 4 show characteristics that would be expected of a statically disordered system through a series of different compositions, if the two atomic centers in disorder—in this case, O(1) from the Cr complex and O(1) from the zinc complex—were quite close to each other. There is a steady change in the magnitudes of the principal displacements, and the orientation of the principal displacements follows a smooth progression. While the behavior of atom O(2) is not as clear-cut, it also shows a progressive change with composition, in terms of the sizes and orientations of the principal displacements. There appears to be room in the crystal structure to accommodate a distorted chromium complex and the zinc complex. A simple calculation for the structure of sample **5** (48% chromium), in which we modified the coordinates of O(1), H(1), and H(2) so that the distance M–O(1) had the value 2.324 Å (the long value in the Cr complex), showed no unreasonable crowding with the nearest sulfate group. We calculated that the hydrogen bond O(1)–H(1)···O(6A) would have O(1)···O(6A) = 2.739 Å, H(1)···O(6A) = 1.996 Å, and O(1)–H(1)···O(6A) = 159°. For the interaction O(1)–H(2)···O(7A), the values would be O(1)···O(7A) = 2.760 Å, H(2)···O(7A) = 2.041 Å, and O(1)–H(2)···O(7A) = 159°. While the combination of short distances and such bent angles do not suggest the best of hydrogen-bonding interactions, these values are within the realm of credibility. We also note that although this calculation was based upon nothing more than a simple elongation of the M–O bond, the displacement parameters actually imply an elongation accompanied by lateral displacement.

This interpretation of the data leaves some questions unanswered. First of all, it does not explain why the Jahn–Teller distortion is switched upon formation of the mixed crystals. Moreover, in a case of static disorder with the congeners separated by 0.2 Å (assuming that upon switching, the Jahn–Teller distortion at Cr keeps its original magnitude), one would not expect to locate and refine the hydrogen atoms easily, as we were able to do with all of the mixed crystals except one. And finally, while it is the displacement parameters, and in particular the ΔMSDA values, that call one's attention to this interpretation of the data, the ΔMSDA values of the oxygen atoms with respect to their hydrogen-bond interactions nicely show the behavior that would be expected of a system without disorder.

Figure 5 shows a contoured section of an "omit map" in the region of atom O(1), for sample **8**. (The omit map is a difference Fourier map computed using F_{calc} from which the contribution of the atom in question is excluded; it is used to identify problems in specific sites in an otherwise complete model.) As the figure shows, the omit map does not imply a double maximum in the electron density in this region, even though a close look actually reveals the transverse distortion of electron density that is more clearly visible in the refined displacement parameters in Figure 4. For a case of static disorder, one would expect a double maximum in the omit map or an extended or poorly defined maximum.

For a case of static disorder, the separation between the congeneric centers would have to be rather small—probably less than 0.1 Å—in order to give all of the effects that we observe.

(b) Fully Dynamic Disorder. If the displacement parameters observed for the mixed crystals were the results of purely dynamic disorder, the accompanying geometrical considerations would be similar to those for the case of static disorder; however the physical implications would be rather different. Dynamic disorder would imply that the positions of the potential energy minima for oxygen atoms attached to chromium were crystallographically equivalent to those for oxygen atoms attached to zinc, even if the shapes of the potential energy functions were different for the two cases. This would further imply that the mean atomic position observed for a given oxygen atom was in fact the same mean position throughout the crystal and not an average of two nearly equivalent mean positions. For dynamic disorder, the shape and orientation of the displacement ellipsoids shown in Figure 4 would be taken as reflections of the potential energy function near the oxygen atom. This interpretation seems to mesh more satisfactorily with the odd angular progression of the principal displacements than would a static-disorder interpretation. This interpretation also appears to agree more closely with the contoured omit map shown in Figure 5. Finally, a case of purely dynamic disorder is consistent in concept with the fact that the ΔMSDA values show an expected trend for hydrogen bonds, even though they indicate significant nonlibrational motion for the transition-metal complex. That is to say, it is conceivable that the Zn and Cr complexes, displaced slightly from their conformational energy minima, could display soft vibrations while the hydrogen-bonding network maintained some degree of rigidity in the intermolecular structure.

This interpretation also leaves some questions open. In particular, while it is quite easy to imagine a hexaaquachromium complex displaced from its potential energy minimum, we would expect the corresponding zinc complex to be less susceptible to distortion by its crystalline surroundings. It also remains true that an interpretation based on dynamic disorder, given the diffraction data presented here, rests more on negative considerations regarding other interpretations than on any positive demonstration of dynamic disorder by the data.

In the jargon of structural chemistry, this situation would not normally be called disorder, but in literature related to the study of displacement parameters, the term "dynamic disorder" is commonly used. We adhere to the latter usage, for the purposes of this study.

(c) Combined Static and Dynamic Disorder. It is clear that the Jahn–Teller effect in the $[Cr(H_2O)_6]^{2+}$ complex has undergone some kind of modulation upon incorporation of this moiety into mixed crystals with the analogous zinc complex. It is not obvious that a zinc complex is flexible enough to compromise its shape upon formation of the mixed crystal. It is possible that the shape of the chromium complex changes upon formation of the crystals but that the systems do not reach such a state of homogeneity that the Cr–O and Zn–O bonds are identical in length throughout a given sample. Given that there is space enough in the surroundings of a molecule for an extra degree of distortion, it is possible that the zinc complex retains some degree of molecular rigidity while the chromium complex oscillates about some point on its conformational energy surface. This notion of a combination of static and dynamic disorder can even be taken to the extreme conclusion that the zinc complex retains its original shape while

the chromium complex oscillates between two equivalent Jahn–Teller distortions—one with Cr–O(1) elongated and one with Cr–O(2) elongated.

The displacement parameters do not lend obvious support to the extreme interpretation of this notion, but they would not contradict, in concept, a conclusion that both types of disorder are present.

(d) Other Considerations. Sample **10**, with $x(Cr) = 0.93$, yielded the only poorly behaved refinement of the 11 samples under study. Given the overall increase in displacement parameters with increasing $x(Cr)$, and given the fact that the chromium end-member is not isotypic with sample **10**, we expect this sample to be less stable than the rest. The displacement parameters do not imply the presence of a nascent Jahn–Teller distortion switch, but it seems that the 93% chromium sample pushes the limits of the ability of solid solution formation to influence the structure of the chromium complex. Again, all of this is consistent with the presence of either static or dynamic effects.

Conclusion. The data presented here for 11 ammonium Cr, Zn, and mixed Cr/Zn Tutton salts demonstrate that the Jahn–Teller effect seen for the chromium end member is significantly modified by incorporation of this complex into crystals that also contain the zinc Tutton salt. These data do not easily distinguish between interpretations based on static disorder, those based on dynamic disorder, and those based on the coexistence of both types of disorder. It is possible to employ other, more intuitive considerations in deciding among the possibilities; but if one adheres rigorously to the results of the diffraction analyses, a proof of one mechanism of solid solution formation in the Tutton salts does not readily emerge.

We have begun a series of physical measurements, to be reported in due course, in order to elucidate the microscopic nature of the mixed crystals.

Acknowledgment. Financial support from the Vicerrectoría de Investigación, University of Costa Rica (Grant No. 115-87-516), the Robert A. Welch Foundation (Grant No. A-494), and the Comisión Interministerial de Ciencia y Tecnología (Spain) (Project PB92-0360) is gratefully acknowledged. We also thank Ms. M. Bravo for assistance with the atomic absorption measurements.

Supplementary Material Available: Tables giving a summary of crystallographic refinement data, complete bond distances and angles (including hydrogen bonds), anisotropic displacement parameters, hydrogen atom parameters, and ΔMSDA values for samples **1–11** (44 pages). Ordering information is given on any current masthead page.